Shading and Colour

Recovery of Illuminant and Surface Colors from Images Based on the CIE Daylight

Yuichi OHTA and Yasuhiro HAYASHI

Institute of Information Sciences and Electronics
University of Tsukuba
Tsukuba,Ibaraki,305,JAPAN

Abstract. We propose a color constancy algorithm suitable for robot vision under natural environments based on the CIE daylight hypothesis. The algorithm can recover the illuminant color and the surface color in the scene from the R, G and B values observed on two color images, typically the current image and the past image. It utilizes the advantage of a robot which can exactly memorize images observed in the past. By employing the CIE daylight as a constraint, the stability and the accuracy of the color constancy algorithm based on multiple images, which we proposed previously, are remarkably improved. Effectiveness of the constraint is examined theoretically by analysing the behaviour of the algorithm under the existence of noise and also experimentally by using synthesized and real color images.

1 Introduction

Color is a useful information for a robot to recognize scenes. However, the color observed through images is often changed by the fluctuation of illumination. It is difficult to use such color as a stable feature in computer vision. On the other hand, human visual system has a function called color constancy and we can identify objects in the scene using color as an important key under the variation in illumination. A computational theory for color constancy has been an important target in computer vision [2] [3] [4] [5] [6] [7] [8] [9]. By realizing a function similar to human color constancy on a robot, color can be used as a stable feature under the uncontrollable illumination in natural environments.

We think that the realization of color constancy on a robot need not to follow the framework to which we human beings are constrained. A robot, or a computer, can exactly memorize image information observed in the past. Therefore, it is reasonable to use not only the image information being observed currently but also the image information observed in the past. That is, the color constancy on a robot can use a framework using multiple images as illustrated in figure 1. By utilizing this advantage, we can realize a computational algorithm which is more general and more accurate than those which follow the restriction of a single image as in the human vision.

We have proposed a color constancy algorithm using multiple images [1]. In this algorithm, when two pairs of objects are identified on two images observed

Lecture Notes in Computer Science, Vol. 801
Jan-Olof Eklundh (Ed.)
Computer Vision – ECCV '94

under different illuminations, the colors of illuminant and the surface reflectance in the scene can be recovered from the R, G and B values observed on the two images. The algorithm does not require any specific assumption on the true color in the scene.

The problem of color constancy is ill-posed, in general, in the sense that it is very difficult to determine the solution stably. The discrepancy between the assumed ideal models and the real data sometimes guides our previous algorithm to inaccurate solutions. In order to use the algorithm in practical situations, it is essential to make the algorithm tough. Based on an error analysis, we found that the major reason for the instability is the too large freedom in the illuminant color space. When the illuminant in a scene is a daylight, it should be close to the CIE daylight illuminant. By using the CIE daylight hypothesis to reduce the freedom in the illuminant color, we have developed a more stable algorithm for recovering colors of illuminant and surface reflectance based on the R, G and B values of color images.

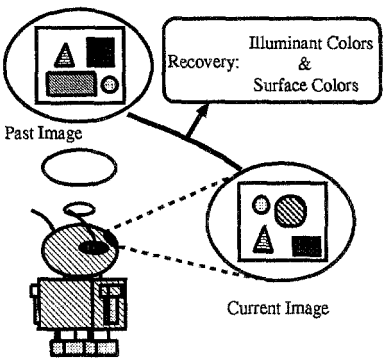

Fig. 1. A framework of color constancy for robot vision

2 Illuminant and Surface Colors from Multiple Images

2.1 A Model for Color Image Acquisition

The process to acquire the three primary components of color image can be summarized as follows. First, the light from the illuminant hits the surface of an object and it is reflected. This reflected light comes into the camera and is decomposed into three primary colors. Each of the three components is converted into an electric signal and is amplified to make the output signal values R, G and B. Thus the R, G and B values of the object are obtained by multiplying the spectral power distribution $E(\lambda)$ of reflected light from the object with the spectral sensitivity of each channel $S_R(\lambda)$, $S_G(\lambda)$ and $S_B(\lambda)$, respectively.

$$R = \int S_R(\lambda)E(\lambda)d\lambda$$

$$G = \int S_G(\lambda)E(\lambda)d\lambda$$
$$B = \int S_B(\lambda)E(\lambda)d\lambda \quad (1)$$

where λ represents the wavelength and they are integrated over the range of visible spectrum. The reflected light $E(\lambda)$ is represented as,

$$E(\lambda) = I(\lambda)R(\lambda) \quad (2)$$

where $I(\lambda)$ is the spectral power distribution of the illuminant, and $R(\lambda)$ is the surface spectral reflectance of the object. When the illuminant changes, the R, G and B values observed on the image are changed even for a same object.

2.2 Models for Illuminant and Surface Reflectance

In order to recover $I(\lambda)$ and $R(\lambda)$ from the R, G and B values in images, they should be modeled with a few parameters. A finite-dimensional linear model is often employed for the purpose [2] [3] [4] [6] [7] [8]. In the model, the spectral property of the illuminant or the surface reflectance is described by a weighted summation of a fixed set of basis vectors.

In order to obtain the basis vectors for surface reflectance, a large number of samples of spectral reflectance should be measured on various materials. Cohen [11] has computed the principal components of 150 samples of Munsell chips randomly selected from a total of 433 chips. In his analysis it turned out the mean and the first two components accounted for 99.18% of the variance of the samples. Parkkinen *et al.* [12] reported a similar result using 1257 samples.

As for the basis vectors for illuminant, Judd *et al.* [10] have examined the spectral distributions of 622 samples from typical daylights. The study showed that the mean and the first two principal components accounted for almost 100% of the variance of the samples.

We, therefore, describe $I(\lambda)$ and $R(\lambda)$ with weighted summation of three basis vectors.

$$\begin{aligned} I(\lambda) &= a_1 I_1(\lambda) + a_2 I_2(\lambda) + a_3 I_3(\lambda) \\ R(\lambda) &= b_1 R_1(\lambda) + b_2 R_2(\lambda) + b_3 R_3(\lambda) \end{aligned} \quad (3)$$

We call the coefficients (a_1, a_2, a_3) and (b_1, b_2, b_3) in equation (3) as the characteristic parameters representing spectral properties of illuminant and surface reflectance, respectively.

2.3 Recovery of Scene Color Using Multiple Images

Equations representing the relations between the R, G and B values and the characteristic parameters of the spectral properties of illuminant and surface

reflectance can be obtained by substituting equations (2) and (3) into equation (1).

$$
\begin{aligned}
R &= \int S_R(\lambda) \sum_{i=1}^{3} a_i I_i(\lambda) \sum_{j=1}^{3} b_j R_j(\lambda) d\lambda \\
&= \sum_{i=1}^{3} \sum_{j=1}^{3} a_i b_j \left\{ \int S_R(\lambda) I_i(\lambda) R_j(\lambda) d\lambda \right\} \\
G &= \int S_G(\lambda) \sum_{i=1}^{3} a_i I_i(\lambda) \sum_{j=1}^{3} b_j R_j(\lambda) d\lambda \\
&= \sum_{i=1}^{3} \sum_{j=1}^{3} a_i b_j \left\{ \int S_G(\lambda) I_i(\lambda) R_j(\lambda) d\lambda \right\} \\
B &= \int S_B(\lambda) \sum_{i=1}^{3} a_i I_i(\lambda) \sum_{j=1}^{3} b_j R_j(\lambda) d\lambda \\
&= \sum_{i=1}^{3} \sum_{j=1}^{3} a_i b_j \left\{ \int S_B(\lambda) I_i(\lambda) R_j(\lambda) d\lambda \right\}
\end{aligned} \tag{4}
$$

We assume that the spectral sensitivities $S_R(\lambda)$, $S_G(\lambda)$ and $S_B(\lambda)$ of the camera are *a priori* known. Since $I_i(\lambda)$s, $R_j(\lambda)$s, $S_R(\lambda)$, $S_G(\lambda)$ and $S_B(\lambda)$ in equation (4) are known, we can compute each of the integral terms in advance. Thus equation (4) can be represented as a set of nonlinear quadratic equations of unknown characteristic parameters $\boldsymbol{a} = (a_1\ a_2\ a_3)^T$ and $\boldsymbol{b} = (b_1\ b_2\ b_3)^T$.

$$
\begin{aligned}
R &= \boldsymbol{b}^T \boldsymbol{S}_R \boldsymbol{a} \\
G &= \boldsymbol{b}^T \boldsymbol{S}_G \boldsymbol{a} \\
B &= \boldsymbol{b}^T \boldsymbol{S}_B \boldsymbol{a}
\end{aligned} \tag{5}
$$

where $\boldsymbol{S}_R$, $\boldsymbol{S}_G$ and $\boldsymbol{S}_B$ are 3×3 constant matrices, and their ijth element is the value of $\int S_R(\lambda) I_i(\lambda) R_j(\lambda) d\lambda$, etc. Now we consider these three equations as the observation equation representing the relation between the six characteristic parameters of scene color and the R, G and B values observed on an image. Let denote them in a simpler form as,

$$
\boldsymbol{C} = \boldsymbol{F}(\boldsymbol{a}, \boldsymbol{b}) \tag{6}
$$

where $\boldsymbol{C} = (R\ G\ B)^T$, and $\boldsymbol{F}()$ represents the set of three quadratic equations.

Now the color constancy problem can be treated as a problem of solving the unknown variables $\boldsymbol{a}$ and $\boldsymbol{b}$ based on equation (6). According to the relationship between the number of equations obtained from images and the number of unknown parameters, the simplest case to solve the equations is that two objects ($\boldsymbol{b}_1$ and $\boldsymbol{b}_2$) are identified on two images observed under two different illuminants

($\boldsymbol{a}_1$ and $\boldsymbol{a}_2$) as shown in equation (7) [1]. Figure 2 illustrates the situation. Both of the number of equations and the number of unknown parameters are twelve.

$$\begin{aligned} \boldsymbol{C}_{11} &= \boldsymbol{F}(\boldsymbol{a}_1, \boldsymbol{b}_1) \\ \boldsymbol{C}_{12} &= \boldsymbol{F}(\boldsymbol{a}_1, \boldsymbol{b}_2) \\ \boldsymbol{C}_{21} &= \boldsymbol{F}(\boldsymbol{a}_2, \boldsymbol{b}_1) \\ \boldsymbol{C}_{22} &= \boldsymbol{F}(\boldsymbol{a}_2, \boldsymbol{b}_2) \end{aligned} \tag{7}$$

where $\boldsymbol{C}_{pq}$ represents the $(R \;\; G \;\; B)^T$ of object q observed under illuminant p.

All terms on the right hand side of equation (7) are the form of $a_i b_j$ as shown in equation (4). This means that unless one of the twelve unknown parameters in equation (7) is fixed, all unknown parameters can not be fixed. In other words, one of the twelve equations in equation (7) is redundant. Therefore we fix a_{11} of $\boldsymbol{a}_1$ to a constant and determine all unknown parameters using a least-square method based on equation (8).

$$\min \left[\sum_{p=1}^{2} \sum_{q=1}^{2} \{\boldsymbol{C}_{pq} - \boldsymbol{F}(\boldsymbol{a}_p, \boldsymbol{b}_q)\}^2 \right] \tag{8}$$

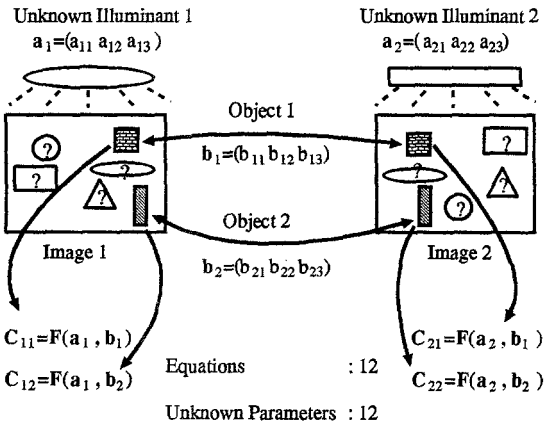

Fig. 2. Recovery of scene colors from two color images

2.4 Error Analysis

The algorithm described in the previous section works fairly well in the "ideal" situation: *i.e.*, the illuminants and the surface reflectances are exactly the summation of three basis vectors and no noise is included in the image acquisition process. In real situations, however, the color information obtained from images is not free of noise. As illustrated in figure 3, noise is included at every step of the image acquisition process. By the existence of such noise, the minimum of equation (8) becomes ambiguous and the stability of the algorithm is lost. In order to analyze the stability of the algorithm, we explicitly describe the noise

factors at each step in figure 3 as follows; illuminant modeling error $\Delta I(\lambda)$, reflectance modeling error $\Delta R(\lambda)$, sensitivity measurement error $\Delta S_R(\lambda)$, $\Delta S_G(\lambda)$ and $\Delta S_B(\lambda)$, and R, G and B values observation error ΔR, ΔG and ΔB.

The non-linear simultaneous equation (7) can be converted to linear simultaneous equations with six unknowns $\boldsymbol{b}_1$ and $\boldsymbol{b}_2$ by fixing the characteristic parameters of illuminants $\boldsymbol{a}_1$ and $\boldsymbol{a}_2$.

$$\boldsymbol{Y}_C = \boldsymbol{A}\boldsymbol{x}_b \tag{9}$$

where $\boldsymbol{Y}_C$ is a 6×2 matrix which has R_{pq}, G_{pq} and B_{pq} values observed for two objects on two images ($p = 1, 2$; $q = 1, 2$), $\boldsymbol{A}$ is a 6×3 matrix whose element is determined by the $\boldsymbol{S}_R$, $\boldsymbol{S}_G$, $\boldsymbol{S}_B$, $\boldsymbol{a}_1$ and $\boldsymbol{a}_2$, and $\boldsymbol{x}_b$ is a 3×2 matrix composed of the unknown characteristic parameters of surface reflectances. When we describe the error explicitly, equation (9) can be written as follows.

$$\boldsymbol{Y}_C + \boldsymbol{\Delta Y}_C = (\boldsymbol{A} + \boldsymbol{\Delta A})(\boldsymbol{x}_b + \boldsymbol{\Delta x}_b) \tag{10}$$

where $\boldsymbol{\Delta Y}_C$ represents errors in the observed data as stated, $\boldsymbol{\Delta A}$ is the variation in $\boldsymbol{A}$ caused by the fluctuation of the characteristic parameters $\boldsymbol{a}_1$ and $\boldsymbol{a}_2$. The fluctuation in the solution is represented as

$$\frac{\|\boldsymbol{\Delta x}_b\|}{\|\boldsymbol{x}_b\|} \leq \left(\frac{\sigma_1}{\sigma_3}\right)\left(\frac{1}{1 - \left(\frac{\sigma_1}{\sigma_3}\right)\frac{\|\boldsymbol{\Delta A}\|}{\|\boldsymbol{A}\|}}\right)\left(\frac{\|\boldsymbol{\Delta Y}_C\|}{\|\boldsymbol{Y}_C\|} + \frac{\|\boldsymbol{\Delta A}\|}{\|\boldsymbol{A}\|}\right) \tag{11}$$

where $\|\cdot\|$ represents norm, σ_1 and σ_3 are the maximum and the minimum singular values of matrix $\boldsymbol{A}$, respectively, and σ_1/σ_3 is called the condition number of matrix $\boldsymbol{A}$. Equation (11) shows that the fluctuation in the $\boldsymbol{b}_1$ and $\boldsymbol{b}_2$ caused by the $\boldsymbol{\Delta Y}_C$ and $\boldsymbol{\Delta A}$ is magnified by the condition number of matrix $\boldsymbol{A}$.

By fixing the characteristic parameters of surface reflectances $\boldsymbol{b}_1$ and $\boldsymbol{b}_2$, equation (7) can be converted into linear simultaneous equations with six unknowns $\boldsymbol{a}_1$ and $\boldsymbol{a}_2$.

$$\boldsymbol{Y}_C = \boldsymbol{B}\boldsymbol{x}_a \tag{12}$$

$\boldsymbol{B}$ is a 6×3 matrix determined by the $\boldsymbol{S}_R$, $\boldsymbol{S}_G$, $\boldsymbol{S}_B$, $\boldsymbol{b}_1$ and $\boldsymbol{b}_2$, and $\boldsymbol{x}_a$ is a 3×2 matrix composed of the unknown characteristic parameters of illuminants. Following the same steps as equation (11), we can obtain equation (13).

$$\frac{\|\boldsymbol{\Delta x}_a\|}{\|\boldsymbol{x}_a\|} \leq \left(\frac{\sigma_1'}{\sigma_3'}\right)\left(\frac{1}{1 - \left(\frac{\sigma_1'}{\sigma_3'}\right)\frac{\|\boldsymbol{\Delta B}\|}{\|\boldsymbol{B}\|}}\right)\left(\frac{\|\boldsymbol{\Delta Y}_C\|}{\|\boldsymbol{Y}_C\|} + \frac{\|\boldsymbol{\Delta B}\|}{\|\boldsymbol{B}\|}\right) \tag{13}$$

where σ_1' and σ_3' are the maximum and the minimum singular values of matrix $\boldsymbol{B}$, respectively, and σ_1'/σ_3' is the condition number of matrix $\boldsymbol{B}$.

We have examined the condition numbers of matrices $\boldsymbol{A}$ and $\boldsymbol{B}$ by setting the characteristic parameters $\boldsymbol{a}$ and $\boldsymbol{b}$ to various values observable in real scenes. Table 1 shows their maximum, minimum, and mean values. In this examination, we used the spectral sensitivities actually measured on a 3CCD-TV camera for the $S_R(\lambda)$, $S_G(\lambda)$ and $S_B(\lambda)$. The basis vectors by Judd are used for $I_i(\lambda)$s. For $R_j(\lambda)$s, basis vectors derived from the actual spectral reflectance of the

color chips on the Macbeth Color Checker [13], which are similar to the vectors by Cohen, are used. It will be clear from table 1 that equation (13) is far more sensitive to noise than equation (11). This means the characteristic parameters of illuminant easily become unstable under the existence of noise and it is necessary to introduce an additional constraint for the illuminant to make the algorithm more stable.

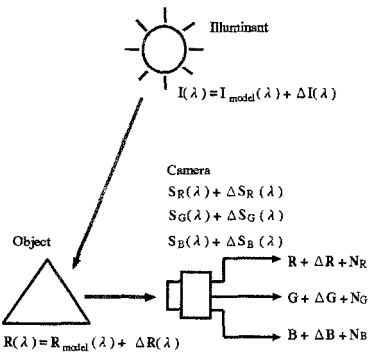

Fig. 3. Noise factors

Table 1. Condition numbers of matrix A and B

	max.	mean	min.
matrix A	2.62	1.54	1.27
matrix B	291.35	89.23	50.62

3 Recovery Based on the CIE Daylight Hypothesis

3.1 The CIE Daylight Hypothesis

In order to improve the stability and the accuracy of the color constancy algorithm by giving an additional constraint to the illuminant color, we introduce the CIE daylight hypothesis.

The CIE daylight hypothesis: "When the illuminant is a daylight, its spectral power distribution should be close to the CIE daylight at a certain color temperature."

The CIE daylight is a model of typical daylights proposed by the CIE (Commission Internationale de l'Eclairage) in 1966 [10], and its spectral distribution depends on a single parameter called color temperature. A relative power distribution $I_{day}(\lambda)$ can be modeled by

$$I_{day}(\lambda) = I_{mean}(\lambda) + M_1 I_{first}(\lambda) + M_2 I_{second}(\lambda) \tag{14}$$

where $I_{mean}(\lambda)$, $I_{first}(\lambda)$ and $I_{second}(\lambda)$ correspond to the mean, the first and the second components obtained by Judd, respectively. M_1 and M_2 are calculated

from the chromaticity coordinates x and y corresponding to the position on the CIE chromaticity chart where the color of the given light would appear.

$$M_1 = \frac{-1.3515 - 1.7703x + 5.9114y}{0.0241 + 0.2562x - 0.7341y}$$
$$M_2 = \frac{0.0300 - 31.4424x + 30.0717y}{0.0241 + 0.2562x - 0.7341y} \tag{15}$$

The chromaticity coordinates in turn can be calculated from a given correlated color temperature T_C as follows.

$$x = -4.6070\frac{10^9}{T_C^3} + 2.9678\frac{10^6}{T_C^2} + 0.09911\frac{10^3}{T_C} + 0.244063 \quad (for\ 4000K \leq T_C < 7000K)$$
$$x = -2.0064\frac{10^9}{T_C^3} + 1.9018\frac{10^6}{T_C^2} + 0.24748\frac{10^3}{T_C} + 0.237040 \quad (for\ 7000K \leq T_C < 25000K)$$
$$y = -3.000x^2 + 2.870x - 0.275 \tag{16}$$

3.2 Recovery Based on The CIE Daylight Hypothesis

The basis vectors $I_1(\lambda)$, $I_2(\lambda)$ and $I_3(\lambda)$ for illuminant color in equation (3) correspond to $I_{mean}(\lambda)$, $I_{first}(\lambda)$ and $I_{second}(\lambda)$ in equation (14), respectively. When we assume $a_1 = 1$, the characteristic parameters (a_2, a_3) correspond to (M_1, M_2) in equation (14). From the equations (15) and (16), the (a_2, a_3) of CIE daylights should be on the curve illustrated in figure 4. Then the difference between an illuminant and the CIE daylight can be measured by the distance $E(\boldsymbol{a})$ on the (a_2, a_3) plane as shown in figure 4. The illuminants recovered by the color constancy algorithm should minimize both of equation (8) and the distance $E(\boldsymbol{a})$ simultaneously. Then we define equation (17) for the target of minimization.

$$\min\left[\sum_{p=1}^{2}\sum_{q=1}^{2}\{\boldsymbol{C}_{pq} - \boldsymbol{F}(\boldsymbol{a}_p, \boldsymbol{b}_q)\}^2 + \alpha\sum_{p=1}^{2}E^2(\boldsymbol{a}_p)\right] \tag{17}$$

where α is a weight.

In order to find the set of parameters which minimize equation (8) and equation (17), we employed the non-linear simplex method [14]. In oder to find a set of 11 parameters which minimizes the objective function, the simplex method generates a general simplex with 12 vertices in the 11 dimensional parameter space. Comparing the function values at the 12 vertices, the vertex with the largest value is replaced with a new vertex by one of the three operations, reflection, contraction and expansion. A unit general simplex with 12 vertices, one of which is located at the origin, is set for the initial simplex and the replacement repeats until the simplex converges. The coefficients for the reflection, the contraction and the expansion are set to 1.0, 0.5 and 2.0, respectively.

4 Experiments

In order to demonstrate the validity of our new algorithm proposed in this paper, experiments using synthesized color images and real color images have been performed. The Macbeth Color Checker was used in both experiments as the color object.

4.1 Experiments with Synthesized Images

The color images used in this experiment are synthesized in the following condition. The two illuminants are the CIE daylights at the color temperatures $4800K$ and $10000K$. In order to simulate the modeling error in the illuminant, the fourth basis vector of Judd, *i.e.*, the vector corresponding to the third component, is added to the ideal CIE daylight. The weight for the fourth vector is controlled to make the error between the synthesized illuminant and the CIE daylight to be 0.1 in the definition of equation (18). The spectral reflectances of objects are the actual measurements from the color chips on the Macbeth Color Checker. The spectral sensitivities of camera are the actual measurements of a 3CCD-TV camera. Two color images which simulate the appearance of the Macbeth Color Checker under the daylights of $4800K$ and $10000K$ are generated. Then four sets of R, G and B values, two color chips on two images, are supplied to the recovering algorithm.

Figure 5 shows a result obtained by using "orange" and "blue" color chips. Figure 5(a) shows the spectral distribution of illuminant at $4800K$ and figure 5(b) shows the spectral reflectance of the "orange" color chip. In each figure, "with" / "without" means the result obtained with / without the CIE daylight hypothesis. In order to quantitatively evaluate the performance of the results, we define the error measure of a spectral function $X(\lambda)$ compared to its true value $X_{true}(\lambda)$ as equation (18).

$$Error = \sqrt{\frac{\int_{400}^{700} \{X_{true}(\lambda) - X(\lambda)\}^2 \, d\lambda}{700 - 400}} \tag{18}$$

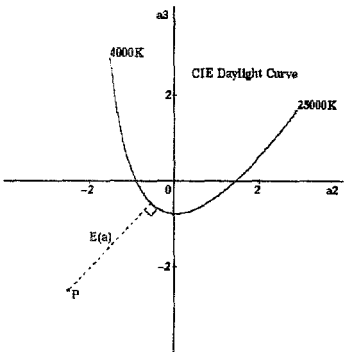

Fig. 4. The CIE daylight curve on the (a_2, a_3) plane and the distance $E(a)$

The results shown in figure 5(a) indicate 0.26 and 0.10 for "without" and "with" cases, respectively. The results shown in figure 5(b) indicate 0.13 and 0.05. In order to examine the influence of the selection of two color chips to the accuracy of the recovered scene colors, the recovery experiments were performed for all the combinations of selecting two color chips from the nineteen chips on the Macbeth Color Checker, *i.e.*, 171 cases. Figure 6 shows the error distribution for recovered colors of illuminant and surface reflectance.

4.2 Experiments with Real Images

We used a monochrome CCD camera with $\gamma = 1$ for the acquisition of R, G and B images. Three color separating filters, No.25, No.58 and No.47, are used for color separation. In order to obtain a good linearity between the input irradiance to the camera and the output R, G and B values, images observed by changing the iris size are combined into an image with a wide dynamic range. We used a lamp which has a spectral power distribution close to a daylight at $6500K$ for the illuminant. An optical filter for color conversion is used to change the color temperature from $6500K$ to $10000K$. The Macbeth Color Checker is illuminated by the lamp with and without the color conversion filter and two sets of RGB images are digitized.

It should be noted that obtaining two images with and without the color conversion filter is a convenience for the experiment and it never means that our algorithm needs more than three different sensor channels as Maloney [8]. The true spectral properties of the lamp, the color conversion filter, and the Macbeth Color Checker are blind to the recovering process, of course, and they are only used to evaluate the accuracy of the results obtained by the color constancy algorithm.

Figure 7 shows the results obtained by using "blue flower" and "moderate red" color chips. Figure 7(a) shows the results for illuminant color at $6500K$ and figure 7(b) shows the results for surface color of "blue flower". The results shown in figure 7(a) have errors of 0.50 and 0.10 defined by equation (18) for "without" and "with" cases, respectively. The results shown in figure 7(b) indicate 0.13 and 0.06. Figure 8 shows the error distribution for recovered illuminant colors and surface colors for the 171 pairs.

5 Conclusion

We proposed a new color constancy algorithm suitable for robot vision based on the CIE daylight. The algorithm uses multiple color images considering the advantage of the robot to the human. The algorithm requires no assumption on the true value of the scene color as the algorithms which use a single image following the human color constancy. By employing the CIE daylight hypothesis for a constraint on the illuminant, the stability and the accuracy of the color constancy algorithm were remarkably improved. We think that the algorithm is effective to recover the scene colors in natural environments.

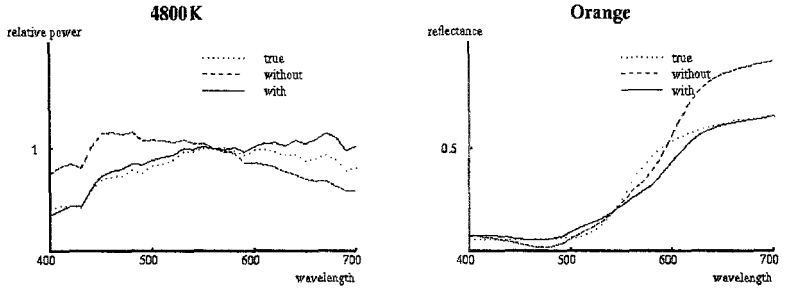

(a): Illuminant color(4800K) (b): Surface color(Orange)

Fig. 5. Results by using synthesized images

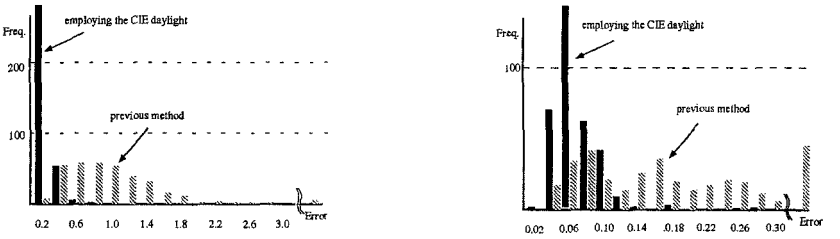

(a): Illuminant color (b): Surface color

Fig. 6. Distribution of recovery error (synthesized images)

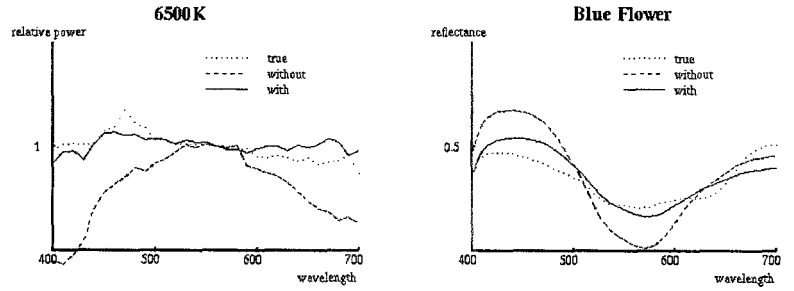

(a): Illuminant color(6500K) (b): Surface color(Blue Flower)

Fig. 7. Results by using real images

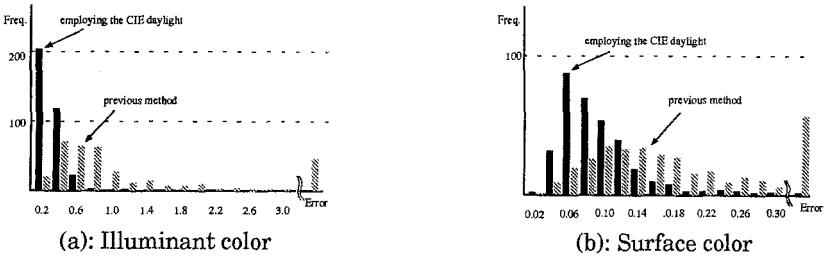

(a): Illuminant color (b): Surface color

Fig. 8. Distribution of recovery error (real images)

Acknowledgments

We appreciate the kindness of Prof. Steven A. Shafer and Miss Carol L. Novak at Carnegie Mellon University who have offered us the spectral data of the Macbeth Color Checker.

References

1. M.Tsukada,Y.Ohta, "An Approach to Color Constancy Using Multiple Images," *IEEE 3rd International Conference on Computer Vision*, pp.385–389,(1990).
2. C.L.Novak,S.A.Shafer, "Supervised Color Constancy Using A Color Chart," *Technical Report CS-90-140,School of Computer Science, Carnegie Mellon University*, (1990).
3. R.Bajcsy,S.W.Lee,A.Leonardis, "Image Segmentation with Detection of Highlights and Inter-reflections Using Color," *Image Understanding and Machine Vision*, Vol.14,pp.16–19(1989).
4. B.Funt,J.Ho, "Color from Black and White," *IEEE 2nd International Conference on Computer Vision*, pp.2–8,(1988).
5. E.Land,J.J.McCann, "Lightness and retinex theory," *J.Opt.Soc.Am.*, 61,pp.1–11,(1971).
6. R.Gershon,A.D.Jepson,J.K.Tsotsos, "From R,G,B to Surface Reflectance: Computing Color Constancy Descriptors in Images," *Proc. of 10th Int. Joint Conf. on Artificial Intelligence*,pp.755 – 758, (1987).
7. G.Buchsbaum, "A Spatial Processor Model for Object Colour Perception," *J.Franklin.Inst.*, 310(1),pp.1–26,(1980).
8. L.T.Maloney,B.A.Wandell, "Color Constancy: a method for recovering surface spectral reflectance," *J.Opt.Soc.Am.*, Vol.3,No.1,pp.29–33,(1986).
9. D.A.Forsyth, "A Novel Algorithm for Color Constancy," *Int. J. Computer Vision*, Vol.5,No.1,pp.5–36,(1990).
10. D.B.Judd,D.L.MacAdam,G.Wyszecki, "Spectral Distribution of Typical Daylight as a Function of Correlated Color Temperature," *J.Opt.Soc.Am.*, Vol.54, No.8, pp.1031 – 1046, (1964).
11. J.Cohen, "Dependency of the spectral reflectance curves of the Munsell color chips," *Psychonomical Science*,Vol.1,pp.369–370,(1964).
12. J.P.S.Parkkinen, J.Hallikainen, T.Jaaskelainen, "Characteristic spectra of Munsell colors," *J.Opt.Soc.Am.A*,Vol.6,No.2,pp.318–322,(1989).
13. C.S.McCamy,H.Marcus,J.G.Davidson, "A Color-Rendition Chart," *Journal of Applied Photographic Engineering*, Vol.2,No.3,pp.95–99,(1976).
14. J.A.Nelder,R.Mead, "A simplex method for function minimization," *The Computer Journal*,Vol.7,pp.308–313,(1965).